INTERNATIONAL JOURNAL FOR NUMERICAL METHODS IN FLUIDS VOL. 21, 295–310 (1995)

NUMERICAL ANALYSIS OF FINITE AMPLITUDE MOTION OF WAVES AND A MOORED FLOATING BODY UNDER SEVERE STORM CONDITIONS

KIYOSHI TAKIKAWA, FUMIHIKO YAMADA, KEIJI SATO AND HIDEKI FURUTA

Department of Civil and Environmental Engineering, Kumamoto University, Kurokami 2-39-1, Kumamoto, Japan

SUMMARY

The motion of a moored floating body under the action of wave forces, which is influenced by fluid forces, shape of the floating body and mooring forces, should be analysed as a complex coupled motion system. Especially under severe storm conditions or resonant motion of the floating body it is necessary to consider finite amplitude motions of the waves, the floating body and the mooring lines as well as non-linear interactions of these finite amplitude motions.

The problem of a floating body has been studied on the basis of linear wave theory by many researchers. However, the finite amplitude motion under a correlated motion system has rarely been taken into account.

This paper presents a numerical method for calculating the finite amplitude motion when a floating body is moored by non-linear mooring lines such as chains and cables under severe storm conditions.

KEY WORDS: moored floating body; finite element method; moving boundary problem

1. INTRODUCTION

We have previously given an analysis of finite amplitude waves on an arbitrary surface of the seabed by the finite element method under coupled motion of the fluid and a floating body,[1] as well as an analysis considering non-linear drag forces caused by the viscosity of the fluid.[2]

This numerical method is divided into three parts as follows.

1. *Analysis of finite amplitude waves on arbitrary surface of seabed.* The finite element method (FEM) is used to solve the boundary problem of the velocity potential satisfying the non-linear free surface boundary condition. A simplified technique for open boundary treatment on a virtual boundary is presented. This numerical method can be easily applied to random as well as regular waves.
2. *FEM analysis for non-linear coupled motion system.* First the velocity potential on the surface of a floating body below sea-level is expressed as a function of the unknown finite displacement of the floating body. Then the solution satisfying conditions of both floating motion and geometry for the surface of the floating body below sea-level is followed successively as an unsteady coupled motion system. Since the momentum equations of the fluid and the floating body are solved at the same time, this numerical method does not require prior calculation of the added

CCC 0271–2091/95/040295–16

Received November 1994
Revised January 1995

mass or the damping force. In contrast, the added mass and the damping force must be considered for the ordinary momentum equation of a floating body.

3. *Numerical analysis for mooring lines subject to non-linear fluid forces.* Unsteady, non-linear analysis of mooring lines subject to a finite amplitude wave force and the reaction force of floating motion is taken into account.

2. ANALYSIS OF FINITE AMPLITUDE WAVES BY FEM

2.1. Fundamental equations

We consider the coupled motion of waves and a floating body in a two-dimensional domain as shown in Figure 1. Assuming the fluid to be incompressible, inviscid and irrotational, the fluid motion can be represented by the velocity potential ϕ. The fluid region $V(\eta)$, which is a function of the free surface displacement, is bounded by the free surface S_1, the rigid bottom boundary S_2, the open boundaries S_3 on the left and right and the floating body's surface S_4 below sea-level. Since the motion of the floating body is a moving boundary problem governed by the Laplace equation in the fluid region $V(\eta)$, the governing field equations and the boundary conditions may be expressed as follows:

(a) in the analytical region $V(\eta)$,

$$\frac{\partial^2\phi}{\partial x^2}+\frac{\partial^2\phi}{\partial y^2}=0, \tag{1}$$

(b) on the free surface S_1,

$$\frac{\partial\phi}{\partial n}=n_y\frac{\partial\phi}{\partial t}, \tag{2}$$

$$\frac{\partial\phi}{\partial t}+\frac{1}{2}\left[\left(\frac{\partial\phi}{\partial x}\right)^2+\left(\frac{\partial\phi}{\partial y}\right)^2\right]+g\eta=0, \tag{3}$$

(c) on the bottom boundary S_2,

$$\frac{\partial\phi}{\partial n}=0, \tag{4}$$

(d) on the open boundaries S_3,

$$\frac{\partial\phi}{\partial n}=\frac{\partial\bar{\phi}}{\partial n}, \tag{5}$$

(e) on the floating body's surface S_4,

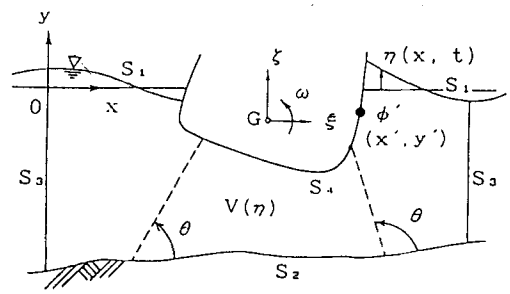

Figure 1. Definition sketch and co-ordinates

$$\frac{\partial \phi}{\partial n} = \frac{\partial \phi'}{\partial n}, \tag{6}$$

where n is the outward normal to the boundaries, n_y is the direction cosine of the normal with respect to the y-axis, $\bar{\phi}$ in (5) is the velocity potential outside the fluid region and the right-side term of (6) is the velocity component normal to the floating body's surface S_4 below sea-level.

2.2. *Variational principle and formulation by FEM*

We can analyse the stationarity conditoin for a functional χ at time t via the following equations from the variational principle with respect to the moving boundary problem:

$$\chi = \frac{1}{2}\iint_{V(\eta)}\left[\left(\frac{\partial \phi}{\partial x}\right)^2 + \left(\frac{\partial \phi}{\partial y}\right)^2\right] dV + \frac{g}{2}\int_{S_1}\eta^2 dS_1 + \int_{S_1}\left(\frac{\partial \phi}{\partial t}\right)\eta\, dS_1 - \int_{S_1}\left(\frac{\partial \eta}{\partial t}\right)\phi\, dS_1 - \int_{S_3}\left(\frac{\partial \bar{\phi}}{\partial n}\right)\phi\, dS_3 - \int_{S_4}\left(\frac{\partial \phi'}{\partial n}\right)\phi\, dS_4, \tag{7}$$

$$\delta\chi = -\iint_{V(\eta)}\left(\frac{\partial^2 \phi}{\partial x^2} + \frac{\partial^2 \phi}{\partial y^2}\right)\delta\phi \cdot dV + \int_{S_1}\left(\frac{\partial \phi}{\partial n} - n_y\frac{\partial \phi}{\partial t}\right)\delta\phi \cdot dS_1 + \int_{S_1}\left\{\frac{\partial \phi}{\partial t} + \frac{1}{2}\left[\left(\frac{\partial \phi}{\partial x}\right)^2 + \left(\frac{\partial \phi}{\partial y}\right)^2\right] + g\eta\right\}\delta\eta \cdot dS_1 + \int_{S_2}\frac{\partial \phi}{\partial n}\delta\phi dS_2 + \int_{S_3}\left(\frac{\partial \phi}{\partial n} - \frac{\partial \bar{\phi}}{\partial n}\right)\delta\phi \cdot dS_3 + \int_{S_4}\left(\frac{\partial \phi}{\partial n} - \frac{\partial \phi'}{\partial n}\right)\delta\phi \cdot dS_4, \tag{8}$$

where the only independent variables are ϕ and η, so $\partial\phi/\partial t$, $\partial\eta/\partial t$, $\partial\phi'/\partial n$ and $\partial\bar{\phi}/\partial n$ are regarded as constants. The velocity potential ϕ can be expressed in equation (9), approximated by linear functions of x and y, if we divide the analytical domain V in time into a set of triangular elements and express the velocity potential ϕ in an element (i, j, m) as the joint value $\mathbf{\Phi} = [\phi_i, \phi_j, \phi_m]$:

$$\mathbf{\Phi} = [N_2, N_j, N_m]\mathbf{\Phi} = [N]\mathbf{\Phi}, \tag{9}$$

$$\frac{\partial \mathbf{\Phi}}{\partial x} = \left[\frac{\partial N}{\partial x}\right]\mathbf{\Phi} = \frac{1}{2\Delta}[b_i, b_j, b_m]\mathbf{\Phi} = \mathbf{B}^{\mathrm{T}}\mathbf{\Phi}, \tag{10}$$

$$\frac{\partial \mathbf{\Phi}}{\partial y} = \left[\frac{\partial N}{\partial y}\right]\mathbf{\Phi} = \frac{1}{2\Delta}[c_i, c_j, c_m]\mathbf{\Phi} = \mathbf{C}^{\mathrm{T}}\mathbf{\Phi}, \tag{11}$$

where, for example, $N_i = (1/2\Delta)(a_i + b_i x + c_i y)$, $a_i = x_j y_m - x_m y_j$, $b_i = y_j - y_m$ and $c_i = x_m - x_j$. The various values of ϕ on the surfaces S_1, S_2, S_3 and S_4 are expressed via the joint value on the boundary of a triangular element as follows:

$$\begin{aligned}
\boldsymbol{\Phi} &= [N_S]\boldsymbol{\Phi}, & \eta &= [N_S]\eta, \\
\frac{\partial \boldsymbol{\Phi}}{\partial t} &= [N_S^*]\left\{\frac{\partial \boldsymbol{\Phi}}{\partial t}\right\}, & \frac{\partial \eta}{\partial t} &= [N_S^*]\left\{\frac{\partial \eta}{\partial t}\right\}, \\
\frac{\partial \bar{\boldsymbol{\Phi}}}{\partial n} &= [N_S^*]\left\{\frac{\partial \bar{\boldsymbol{\Phi}}}{\partial n}\right\}, & \frac{\partial' \boldsymbol{\Phi}'}{\partial n} &= [N_S^*]\left\{\frac{\partial \boldsymbol{\Phi}'}{\partial n}\right\},
\end{aligned} \tag{12}$$

where $[N_s] = [N_i, N_m]$, $[N_s^*] = [N_i^*, N_m^*]$ and the superscript asterisk indicates a value without variation. Therefore equation (7) can be expressed as the joint value of a finite number of elements and we obtain the following equations by applying the variational principle and stationarity condition for $\delta\phi$ and $\delta\eta$:

$$\sum_V (\mathbf{B}\mathbf{B}^{\mathrm{T}} + \mathbf{C}\mathbf{C}^{\mathrm{T}})\boldsymbol{\Phi} \cdot \Delta - \sum_{S_1} \mathbf{S}^* \left\{\eta_y \frac{\partial \eta}{\partial t}\right\} - \sum_{S_3} \mathbf{S}^* \left\{\frac{\partial \bar{\boldsymbol{\Phi}}}{\partial n}\right\} - \sum_{S_4} \mathbf{S}^* \left\{\frac{\partial \boldsymbol{\Phi}'}{\partial n}\right\} = 0, \tag{13}$$

$$\frac{1}{2}\frac{\partial}{\partial \eta}\left(\sum_V \boldsymbol{\Phi}^{\mathrm{T}}(\mathbf{B}\mathbf{B}^{\mathrm{T}} + \mathbf{C}\mathbf{C}^{\mathrm{T}})\boldsymbol{\Phi} \cdot \Delta\right) + \frac{g}{2}\frac{\partial}{\partial \eta}\left(\sum_{S_1} \boldsymbol{\eta}^{\mathrm{T}}\mathbf{S}\boldsymbol{\eta}\right) + \frac{\partial}{\partial \eta}\left(\sum_{S_1} \boldsymbol{\eta}^{\mathrm{T}}\mathbf{S}^* \left\{\frac{\partial \boldsymbol{\Phi}}{\partial t}\right\}\right) = 0, \tag{14}$$

where

$$\mathbf{S} = \int_e [N_s]^{\mathrm{T}}[N_s]\mathrm{d}S, \qquad \mathbf{S}^* = \int_e [N_s]^{\mathrm{T}}[N_s^*]\mathrm{d}S. \tag{15}$$

However, the analytical domain is a function of the independent variational function η and the body's surface below sea-level is a function of the displacement due to the body's motion (Figure 2). Thus the boundaries S_1 and S_4 are functions of the unknown displacement and we have to solve non-linear simultaneous equations; namely, if nth-order approximations at time t are known, then $(n+1)$th-order approximations follow as

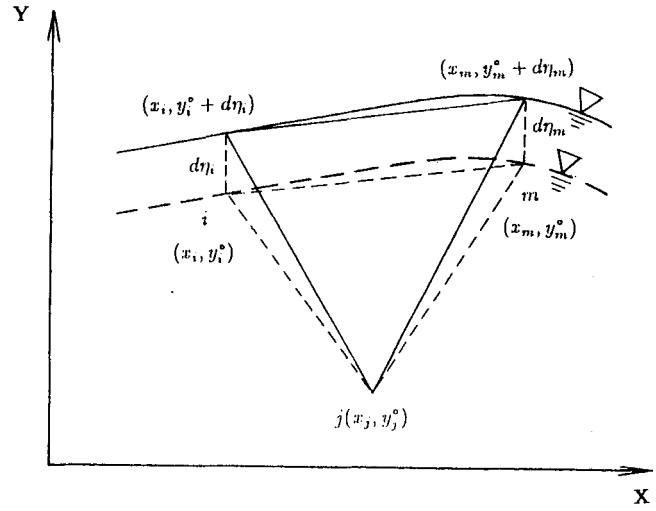

Figure 2. Elements on free surface

$$\begin{aligned} \boldsymbol{\Phi}^{n+1} &= \boldsymbol{\Phi}^n + \mathrm{d}\boldsymbol{\Phi} \equiv \boldsymbol{\Phi}_0 + \mathrm{d}\boldsymbol{\Phi}, \\ \eta^{n+1} &= \eta^n + \mathrm{d}\eta \equiv \eta_0 + \mathrm{d}\eta. \end{aligned} \tag{16}$$

Accordingly, the non-linear shape functions **B**, **C**, **S** and **S*** are corrected as

$$\begin{aligned} &\mathbf{B} = \mathbf{B}_0 + \mathbf{B}_1\,\mathrm{d}\eta, \qquad \mathbf{C} = \mathbf{C}_0 + \mathbf{C}_1\,\mathrm{d}\eta, \\ &\mathbf{S} = \tfrac{1}{3}(l_0 + \mathbf{L}_1^{\mathrm{T}}\,\mathrm{d}\eta)(\mathbf{S}_0 + \mathbf{N}_1\,\mathrm{d}\eta\mathbf{S}_1 + \mathbf{N}_1\mathrm{d}\eta\mathbf{N}_1\,\mathrm{d}\eta\mathbf{S}_3), \\ &\mathbf{S}^* = (l_0/3)(\mathbf{S}_0 + \mathbf{N}_1, \mathrm{d}\eta\mathbf{S}_1 + \mathbf{L}_1^{\mathrm{T}}\,\mathrm{d}\eta\mathbf{S}_0/l_0), \end{aligned} \tag{17}$$

where

$$\mathbf{B}_0^{\mathrm{T}} = \frac{1}{2\Delta_0}[b_i^0, b_j^0, b_m^0] \quad (b_i^0 = z_j^0 - z_m^0, b_j^0 = z_m^0 - z_i^0, b_m^0 = z_i^0 - z_j^0),$$

$$\mathbf{C}_0^{\mathrm{T}} = \frac{1}{2\Delta_0}[c_i, c_j, c_m],$$

$$\mathbf{B}_1 = \frac{1}{2\Delta_0}\begin{bmatrix} -\frac{1}{2\Delta_0}b_i^0 c_i & 1 - \frac{1}{2\Delta_0}b_i^0 c_j & -1 - \frac{1}{2\Delta_0}b_i^0 c_m \\ -1 - \frac{1}{2\Delta_0}b_j^0 c_i & -\frac{1}{2\Delta_0}b_j^0 c_j & 1 - \frac{1}{2\Delta_0}b_j^0 c_m \\ 1 - \frac{1}{2\Delta_0}b_m^0 c_i & -1 - \frac{1}{2\Delta_0}b_m^0 c_j & -\frac{1}{2\Delta_0}b_m^0 c_m \end{bmatrix},$$

$$\mathbf{C}_1 = \frac{-1}{(2\Delta_0)^2}\begin{bmatrix} c_i c_i & c_i c_j & c_i c_m \\ c_j c_i & c_j c_j & c_j c_m \\ c_m c_i & c_m c_j & c_m c_m \end{bmatrix},$$

$\mathbf{N}_1^{\mathrm{T}} = [c_i, c_m]$, $\mathbf{L}_1^{\mathrm{T}} = (b_j/l_0)[-1, 1]$ and l_0 is the nth-order approximate length of the line $\overline{im}$. In addition, in the set of equations obtained by substituting equations (17) into equations (13) and (14), the higher-order terms of $\mathrm{d}\phi$ and $\mathrm{d}\eta$ can be neglected. For the time terms we employ a finite difference method which uses the Heaviside function θ, where the superscript k denotes the value at time $t - \Delta t$:

$$\frac{\partial\phi}{\partial t} = \frac{1}{\theta\Delta t}(\phi^{n+1} - \phi^k) - \frac{1-\theta}{\theta}\left(\frac{\partial\phi}{\partial t}\right)^k, \quad 0 \leqslant \theta \leqslant 1. \tag{18}$$

We employ the same time finite difference method for $\partial\eta/\partial t$. The boundary S_3 is an open boundary on the right and left which is set up in the fluid; the motion of the fluid has to be continuous inside and outside this open boundary. Here we employ a method which satisfies the continuity of mass flux and energy flux with computational time on S_3.[3,4]

2.3. *Open boundary treatment*[5]

A particular concern is the open boundary treatment of finite amplitude waves at the boundary S_3, which uses the mass flux and energy flux because of the continuity of fluid motion. This numerical open boundary method can be easily applied to random as well as regular waves.

As shown in Figure 1, in general the input flow open boundary S_3 has a known incident wave and an unknown reflected wave, while the output flow open boundary has an unknown transmissive wave. For the case of a small-amplitude wave the unknown function at the input and output open boundaries is

defined and can be analysed as for the periodic case. However, for the case of a finite amplitude wave, because it is very difficult to define the general form of wave components exactly, it is necessary to treat the problem as an unsteady one. Each open boundary S_3 is an imaginary boundary established in the fluid; the motion of the fluid has to be continuous inside and outside this boundary.

Here we describe a method of analysis which deals with the vertical distribution of velocity at the imaginary boundary as a function of the surface displacement while satisfying the continuity of mass flux and energy flux on the surface of the imaginary boundary with time, under the condition of continuous motion of the fluid in the domain of analysis of the imaginary boundary.

We express the velocity potential $\bar{\phi}$ at the input and output flow open boundaries S_3 as the summation of an infinite number of component waves on the left and right of boundary S_3 as follows:

$$\bar{\phi}_{\text{inp}} = \sum^{\infty} \bar{\phi}_{il} + \sum^{\infty} \bar{\phi}_{rm}, \qquad \bar{\phi}_{\text{out}} = \sum^{\infty} \bar{\phi}_{tn} \qquad (l, m, n = 1, 2, 3, \ldots), \tag{19}$$

where $\bar{\phi}_{il}$, $\bar{\phi}_{rm}$ and $\bar{\phi}_{tn}$ denote the l-, m- and n-components of the incident, reflected and transmissive waves at any time respectively. Although $\bar{\phi}_{il}$ is a known quantity, since the reflected and transmissive waves represent an unlimited set of unknown quantities, we cannot analyse the problem as it stands. Therefore we select representative waves $\bar{\phi}_r$ and $\bar{\phi}_t$ in each propagation direction and express the unknown terms of (19) approximately as

$$\begin{aligned} \sum^{\infty} \bar{\phi}_{rm} &= \bar{\phi}_r \sum^{\infty} \left(\frac{\bar{\phi}_{rm}}{\bar{\phi}_r} \right) \equiv \bar{\phi}_r R_r = \frac{\sigma_r}{k_r} \frac{\cosh[k_r(h_i + y)]}{\sinh(k_r h_i)} A_r, \\ \sum^{\infty} \bar{\phi}_{tn} &= \bar{\phi}_t \sum^{\infty} \left(\frac{\bar{\phi}_{tn}}{\bar{\phi}_t} \right) \equiv \bar{\phi}_t R_t = \frac{\sigma_t}{k_t} \frac{\cosh[k_t(h_i + y)]}{\sinh(k_t h_i)} A_t. \end{aligned} \tag{20}$$

These equations denote 'the wave of the sum total' of component waves in each propagation direction and deal with this wave represented by a wave which has an unknown constant approximately.

When the continuity at boundary S_3 is introduced into the functional χ, the corresponding values of $\partial\phi/\partial n$ in (7) are given as

$$\begin{aligned} \left(\frac{\partial \bar{\phi}}{\partial n} \right)_{\text{inp}} &= l_{xi} \left(\sum_i \sigma_{il} \frac{\cosh[k_{il}(h_i + y)]}{\sinh(k_{il} h_i)} \eta'_{il} - \sigma_{il} \frac{\cosh[k_r(h_i + y)]}{\sinh(k_r h_i)} A'_r \right), \\ \left(\frac{\partial \bar{\phi}}{\partial n} \right)_{\text{out}} &= l_{xt} \sigma_i \frac{\cosh[k_t(h_i + y)]}{\sinh(k_t h_i),} A'_i, \end{aligned} \tag{21}$$

$$A'_t = \eta_{\text{out}} = (\eta_0 + \mathrm{d}\eta)_{\text{out}}, \tag{22}$$

where the boundary S_3 is kept parallel to the y-axis, l_{xi} and l_{xt} are the direction cosines of the normal drawn outwardly with respect to the x-axis, h_i and h_t are the depths of water at each position and k and σ of each wave satisfy the dispersion equation.

Moreover, η_i denotes the free surface displacement of the incident component wave and is known, while A'_r is the unknown variable of the reflected wave. A'_t is the free surface displacement of the transmissive wave; this unknown is expressed by the free surface displacement η_{out} at the transmissive position via (22). This is equivalent to using the first term of Dean's streamfunction to estimate the inner velocity from the free surface displacement record. A'_r is the only new unknown variable here with regard to the imaginary boundary.

Thus we consider the continuity condition of the energy flux $-\rho(\partial\phi/\partial t)$ $(\partial\phi/\partial n)$ as a new

condition in order to determine the unknown variable. This condition $\int(\partial\phi/\partial t)\mathrm{d}S_3 = \int(\partial\bar{\phi}/\partial t)\mathrm{d}S_3$ is represented at the input flow open boundary as

$$\sum_{S_{3,\mathrm{inp}}} \bar{S}\left(\frac{\partial\phi}{\partial t}\right) = -\sum_i \frac{\sigma_{il}^2}{k_{il}} \frac{\sinh[k_{il}(h_i+\eta_0)]}{\sinh(k_{il}h_i)}\eta'_{il} - \frac{\sigma_r^2}{k_r}\frac{\sinh[k_r(h_i+\eta_0)]}{\sinh(k_r h_i)}A'_r. \tag{23}$$

By considering the continuity conditions (21) and (22) and equation (23) for the motion of the fluid at boundary S_3 and calculating them and the equation which has already been introduced in (7) simultaneously, we can get simultaneous equations of many dimensions which relate $\mathrm{d}\bar{\phi}$, $\mathrm{d}\bar{\eta}$ and A'_r as the unknown variable. By adding a proper basic condition to these equations, we can calculate the unsteady motion of the finite amplitude waves in optional forms or at optional boundary domains which correspond to the incident waves being considered. The method stated above for the imaginary boundary S_3 can be applied not only to regular but also to irregular waves. Moreover, at the boundary S_3, for the case of incident waves produced by the motion of a wave-making plate or the like, by adding the velocity to them according to (21) at the corresponding position, we can also calculate these.

3. ANALYSIS FOR NON-LINEAR COUPLED MOTION SYSTEM

3.1. Condition of floating body's surface below sea-level

We can analyse the motion of the fluid if the velocity condition of the floating body's surface below sea-level, $\partial\phi'/\partial n$, is given. We define the co-ordinates of the centre of gravity of the floating body at rest as $\mathrm{G}(\bar{x}_\mathrm{G}, \bar{y}_\mathrm{G})$ and we define the displacements due to swaying, heaving and rolling motions from the stationary points as ξ, ζ and ω respectively. Since the co-ordinates of the surface of the floating body below sea-level are a function of these displacements, ϕ' can be expressed as

$$\phi'(x', y', t) = \phi'(f(\xi,\omega), g(\zeta,\omega), t). \tag{24}$$

In the analysis of the problem of wave occurrence due to the body's compulsory motion, ξ, ζ and ω in the above equation are known. Accordingly, we can use the same method as before, since $\partial\phi'/\partial n$ is given according to the body's displaced position. On the other hand, in the case where the motion system is influenced by interactions between the wave and the body, the details are as follows. Figure 3 shows an element of the surface below sea-level. When the node (i, j) is displaced by $(\mathrm{d}x, \mathrm{d}y)$ from the nth-order approximation, the increment of the triangular area (i, j, m) is

$$\Delta = \Delta_0 + \tfrac{1}{2}[b_i^0, b_j^0, b_m^0]\mathrm{d}\mathbf{x} + \tfrac{1}{2}[c_i, c_j, c_m]\mathrm{d}\mathbf{y}, \tag{25}$$

where $\mathrm{d}\mathbf{x}^\mathrm{T} = [\mathrm{d}x_i, \mathrm{d}x_j, 0]$ and $\mathrm{d}\mathbf{y}^\mathrm{T} = [\mathrm{d}y_i, \mathrm{d}y_j, 0]$. Now $\partial\phi'/\partial n$ is calculated via

$$\begin{aligned}
\frac{\partial\boldsymbol{\Phi}'}{\partial\mathbf{x}} &= \mathbf{B}^\mathrm{T}\boldsymbol{\Phi}' = (\mathbf{B}_0^\mathrm{T} + \mathrm{d}\mathbf{x}^\mathrm{T}\mathbf{B}_2^\mathrm{T} + \mathrm{d}\mathbf{y}^\mathrm{T}\mathbf{B}_1^\mathrm{T})(\boldsymbol{\Phi}'_0 + \mathrm{d}\boldsymbol{\Phi}'),\\
\frac{\partial\boldsymbol{\Phi}'}{\partial\mathbf{y}} &= \mathbf{C}^\mathrm{T}\boldsymbol{\Phi}' = (\mathbf{C}_0^\mathrm{T} + \mathrm{d}\mathbf{x}^\mathrm{T}\mathbf{C}_2^\mathrm{T} + \mathrm{d}\mathbf{y}^\mathrm{T}\mathbf{C}_1^\mathrm{T})(\boldsymbol{\Phi}'_0 + \mathrm{d}\boldsymbol{\Phi}'),
\end{aligned} \tag{26}$$

where

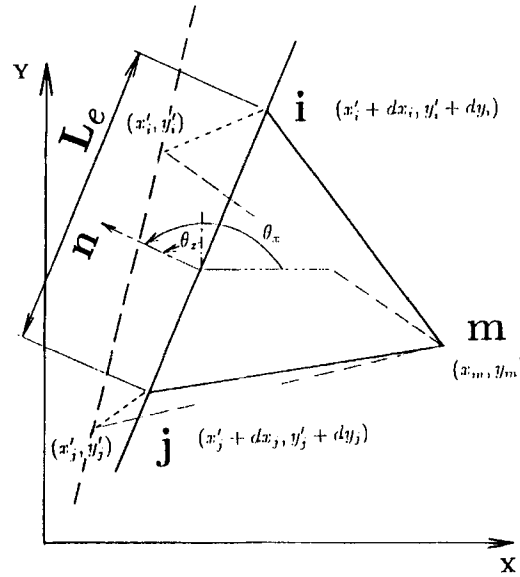

Figure 3. Elements on floating body's surface below sea-level

$$\mathbf{B}_2 = \frac{-1}{(2\Delta_0)^2}\begin{bmatrix} b_i b_i & b_i b_j & b_i b_m \\ b_j b_i & b_j b_j & b_j b_m \\ b_m b_i & b_m b_j & b_m b_m \end{bmatrix}, \qquad \mathbf{C}_2 = \mathbf{B}_1. \tag{27}$$

In equation (25), (**dx**, **dy**) is determined by the displacement of the body. When a point $(\bar{x}, \bar{y})$ apart from the gravity centre G of the floating body at rest moves to the point $(\bar{x}', \bar{y}')$ with the motion of the floating body, it is expressed as

$$\begin{aligned} x' &= \bar{x}_G + \xi + \bar{x}\cos\omega - \bar{y}\sin\omega \equiv x_0' + \mathrm{d}x', \\ y' &= \bar{y}_G + \zeta + \bar{x}\sin\omega + \bar{y}\cos\omega \equiv y_0' + \mathrm{d}y', \end{aligned} \tag{28}$$

Besides, by employing the incremental method, $(n+1)$th-order approximations are expressed by nth-order approximate solutions $(\xi_0, \zeta_0, \omega_0)$ plus increments $(\mathrm{d}\xi, \mathrm{d}\zeta, \mathrm{d}\omega)$, so we obtain

$$\begin{aligned} \mathrm{d}x' &= \mathrm{d}\xi - (\bar{x}\sin\omega_0 + \bar{y}\cos\omega_0)\mathrm{d}\omega, \\ \mathrm{d}y' &= \mathrm{d}\zeta + (\bar{x}\cos\omega_0 - \bar{y}\sin\omega_0)\mathrm{d}\omega. \end{aligned} \tag{29}$$

From the foregoing theory the relations between ϕ' of the floating body's surface below sea-level and the finite displacements of the motion of the floating body are given. The velocity of the floating body's surface below sea-level, $\partial\phi'/\partial n$ is expressed as

$$\frac{\partial\phi'}{\partial n} = \frac{\partial x'}{\partial t} l_x + \frac{\partial y'}{\partial t} l_y, \tag{30}$$

where l_x and l_y are the direction cosines of the normal to the floating body's surface below sea-level with respect to the x- and y-axis respectively. By substituting (29) in (30), $\partial\phi'/\partial n$ can be expressed as a function of the motion velocity of the gravity centre of the floating body $(\mathrm{d}\xi/\mathrm{d}t, \mathrm{d}\zeta/\mathrm{d}t, \mathrm{d}\omega/\mathrm{d}t)$. Therefore we regard the displacements of the gravity centre of the floating body $(\mathrm{d}\xi, \mathrm{d}\zeta, \mathrm{d}\omega)$ as the new unknown displacements. In employing the foregoing theory, we should analyse the following equation of motion of the floating body at one time. Here the geometric conditions of the floating

body's form are satisfied by employing $x' = x_0' + \mathrm{d}x'$ and $y' = y_0' + \mathrm{d}y'$ from the computational results.

3.2. *Momentum equations of floating body*

The momentum equations of the floating body in each direction are expressed as

$$\begin{aligned} M\frac{\mathrm{d}^2\xi}{\mathrm{d}t} &= \int_{S_4} p_{\mathrm{H}}\,\mathrm{d}S_4 - F_{\mathrm{H}} = F_{\mathrm{DH}}, \\ M\frac{\mathrm{d}^2\zeta}{\mathrm{d}t} &= \int_{S_4} p_{\mathrm{V}}\,\mathrm{d}S_4 - F_{\mathrm{V}} + F_{\mathrm{DV}} - (Mg + T_{\mathrm{V}}), \\ I\frac{\mathrm{d}^2\omega}{\mathrm{d}t} &= \int_{S_4} p_{\mathrm{M}}\,\mathrm{d}S_4 - F_{\mathrm{M}} + F_{\mathrm{DM}}, \end{aligned} \tag{31}$$

where M is the mass of the floating body, I is the moment of inertia, F_{H}, F_{V} and F_{M} are the reaction terms of the mooring lines, T_{V} is the vertical component of the mooring forces at rest, p_{H}, p_{V} and p_{M} are the horizontal and vertical components of the fluid pressure and the moment of the fluid pressure acting on the gravity centre of the floating body respectively and F_{DH}, F_{DV} and F_{DM} are the components of the non-linear drag forces caused by the viscosity of the fluid.

The normal fluid pressure p on the floating body's surface below sea-level at (x', y') can be expressed in terms of the velocity potentials as

$$p(x', y') = -\rho\left(\frac{\partial\phi}{\partial t} + \tfrac{1}{2}(\phi_x^2 + \phi_y^2) + gy'\right), \tag{32}$$

where $\phi_x = \partial\phi/\partial x$ and $\phi_y = \partial\phi/\partial y$. By employing (32), we can express the pressure components as $p_{\mathrm{H}} = pl_x$, $p_{\mathrm{V}} = pl_y$ and $p_{\mathrm{M}} = pe$ (where e is the distance of eccentricity between the gravity centre and the point (x', y')).

The drag forces caused by the viscosity of the fluid are expressed as a function of the difference between the particle velocity u and the velocity of the floating body motion, v:

$$F_{\mathrm{D}} = \frac{\rho C_{\mathrm{D}} S V|V|}{2}, \tag{33}$$

where $V = u - v$, C_{D} is the drag force factor and S is the area of projection. This is explained in more detail in Reference 2.

3.3. *Reaction forces of non-linear mooring lines*

If the mooring lines are linear, such as springs, their reaction forces can be expressed in terms of θ in Figure 1 as

$$\begin{aligned} &F_{\mathrm{H}} = K\Delta l\cos\theta, \qquad F_{\mathrm{V}} = K\Delta l\sin\theta, \\ &F_{\mathrm{M}} = (y_{\mathrm{G}} - y_{\mathrm{A}})F_{\mathrm{H}} + (x_{\mathrm{A}} - x_{\mathrm{G}})F_{\mathrm{V}}, \end{aligned} \tag{34}$$

where K is the coefficient of spring stiffness and Δl is the increment of the mooring line (a function of the setting point of the mooring line).

However, if the mooring lines are non-linear, such as cables, we have to analyse for non-linear mooring lines at each computational step. Because of the displacement of the setting point, the reaction forces of mooring lines and the mooring lines themselves are non-linear. Here we employ catenary theory and the lumped mass method.

3.3.1. Catenary theory. We consider the displacements of the setting points of lines moored to a floating body and the extensibility of the lines by catenary theory using the static equilibrium equation. However, we cannot take these into account as they stand, because the displacements of the setting points themselves are finite and unknown. Therefore we employ the incremental method and deal with them linearly. Concerning the setting point A of mooring lines and the position of the gravity centre G of the floating body shown in Figure 4, we can express the unknown $(n+1)$th-order approximations in terms of increments to nth-order approximations known at time t. Then the reaction forces of the mooring lines at this time are expressed as

$$F(x_0 + \mathrm{d}x, y_0 + \mathrm{d}y) = F(x_0, y_0) + \mathrm{d}F(\mathrm{d}x, \mathrm{d}y). \tag{35}$$

When we take up to first-order terms in a Taylor expansion around nth-order approximations, the displacement (dx, dy) of setting point A and the increment of reaction forces (dF_x, dF_y of mooring lines are expressed as

$$\begin{aligned} \mathrm{d}F_x &= C_{xx}\,\mathrm{d}x + C^*_{yx}\,\mathrm{d}y, \\ \mathrm{d}F_y &= C^*_{xy}\,\mathrm{d}x + C_{yy}\,\mathrm{d}y, \end{aligned} \tag{36}$$

where C_{xx} is a linear spring constant of catenary theory[6] and $C^*_{xy} = C^*_{xy}$; the superscript asterisk indicates a difference in sign between the weather side (WS) and the lee side (LS). These linear spring constants differ between the taut and slack states of mooring lines and therefore have to be taken into account in the analysis. The reaction forces of mooring lines in (31) are expressed as

$$\begin{aligned} F_{\mathrm{H}} &= (F_x)_0 + \mathrm{d}F_x, \qquad F_{\mathrm{V}} = (F_y)_0 + \mathrm{d}F_y, \\ F_{\mathrm{M}} &= (y_{\mathrm{G}} - y_{\mathrm{A}})F_{\mathrm{H}} + (x_{\mathrm{A}} - x_{\mathrm{G}})F_{\mathrm{V}}, \end{aligned} \tag{37}$$

where $(F_x)_0$ and $(F_y)_0$ are nth-order approximations. The setting point displacement (dx, dy) is expressed by the displacement of the gravity centre of the floating body as shown in (29), so we can analyse it because the reaction forces of mooring lines are a function of (dξ, dζ, dω).

3.3.2. Lumped mass method. When the motion of the floating body is large, such as under severe storm conditions and close to the point of resonance motion of the floating body, we cannot neglect the motions of the mooring lines themselves and the drag forces working there, so we have to analyse the dynamic condition. There is a method available that takes into account the motion of mooring lines by catenary theory.[7] However, as shown in Figure 5, we instead divide the mooring lines into line

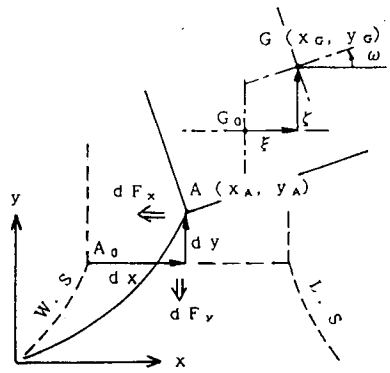

Figure 4. Cables and co-ordinate system for motion of floating body

elements and perform the dynamic analysis by the finite element method (FEM), treating these elements as the motions of a mass system with concentrated mass.

Referring to Figure 5, the equations of motion and the equation of geometric conditions are expressed as

$$\begin{aligned} T_i \cos \phi_i - T_{i-1} \cos \phi_{i-1} + p_{xi} &= m_i \ddot{x}_i, \\ T_i \sin \phi_i - T_{i-1} \sin \phi_{i-1} + p_{yi} - W_i &= m_i \ddot{y}_i, \end{aligned} \tag{38}$$

$$(x_{i+1} - x_i)^2 + (y_{i+1} - y_i)^2 - S_i^2(1 + T_i/AE) = 0 \equiv \psi_i, \tag{39}$$

where p_{xi} and p_{yi} are the components of the fluid forces acting on the mass in the x- and y-direction respectively. They are connected with the fluid forces $p_{\tau i}$ and $p_{\eta i}$ in the local co-ordinates (τ, η) of mooring lines by

$$\begin{aligned} p_{xi} &= p_{\tau i} \cos \phi_{ai} + P_{\eta i} \sin \phi_{ai}, \\ p_{yi} &= p_{\tau i} \sin \phi_{ai} + P_{\eta i} \cos \phi_{ai}, \end{aligned} \tag{40}$$

We varied the acceleration terms of (38) with time and arranged (39) about tensions T to give

$$\{-\psi_i\} = \left[\frac{\partial \psi_i}{\partial T_{i-1}}, \frac{\partial \psi_i}{\partial T_i}, \frac{\partial \psi_i}{\partial T_{i+1}}\right] \begin{Bmatrix} \mathrm{d}T_{i-1} \\ \mathrm{d}T_i \\ \mathrm{d}T_{i+1} \end{Bmatrix}. \tag{41}$$

First we give the setting point position of mooring lines at time t as the boundary condition; secondly we revise the tensions in the above equation by using nth-order approximations for mooring lines; finally we look for $(n+1)$th-order approximations one by one.

4. NUMERICAL RESULTS AND DISCUSSION

The models and experimental conditions for experiment and computation are a floating body moored by cross-springs or cross-chains with two-dimensional rectangular cross-section, as shown in Figures 6 and 7 respectively.

Figure 8 shows the time history of the amplitude ratio ζ/a between the vertical amplitude of motion of the floating body, ζ, and the amplitude of the incident wave, a, when the floating body is moored by cross-chains as in Figure 7, assuming a wave period $T = 1{\cdot}61$ s. The experimental results relate to the

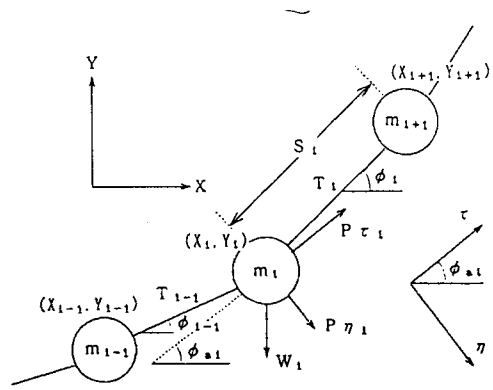

Figure 5. External forces and co-ordinate system acting on concentrated mass

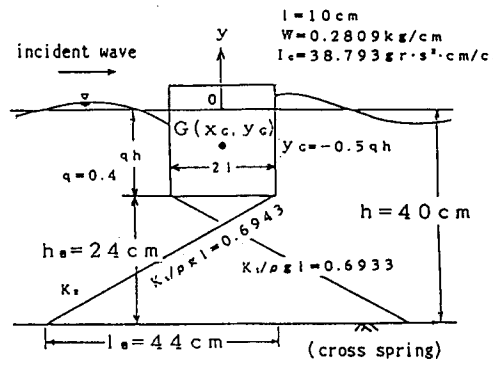

Figure 6. Floating body moored by cross-springs

method corresponding to the VTR scene, while the present numerical solutions relate to the method of analysing mooring lines approximately by catenary theory, with the analysis performed under the condition near the resonance point of the motion of the floating body. The present numerical solutions, although slightly larger than the experimental data since they neglect the drag force terms of the motion of the floating body, agree very well with the experimental results.

Figure 9 shows the present numerical solutions and the experimental results as an average of the time history of tensions when the upper edges of the cross-chains are vibrated by compulsion, i.e. dynamic analysis of the mooring lines. Here each chain of length $S = 115$ cm and unit weight 2·317 gf cm^{-3} is vibrated horizontally on the upper edge with amplitude 1·6 cm. In the dynamic analysis of the cross-chains we take into account only the vertical component of drag and use the coefficient of drag forces $C_D = 1{\cdot}8$ and the coefficient of added mass $C_m = 2{\cdot}0$. The present numerical solutions, although a little smaller than the experimental results, show very good agreement, because the difference is due only to the value of the coefficient of drag forces.

Figure 10 shows the numerical results for the time history of the velocity fields around the floating body by the present analysis for the floating body moored by cross-chains. We calculated the mooring lines by catenary theory one by one. First, the finite amplitudes of the free surface displacements and the floating body's motion are seen. Secondly, the taut state (NT in Figure 10) and the slack state are apparent and the situation related to the centre of the corner is clearly evident. These numerical results agree well with the experiments.

Figure 11 shows the time history of motion (ratios ξ/a, ζ/a and ω/a) of the centre of the floating

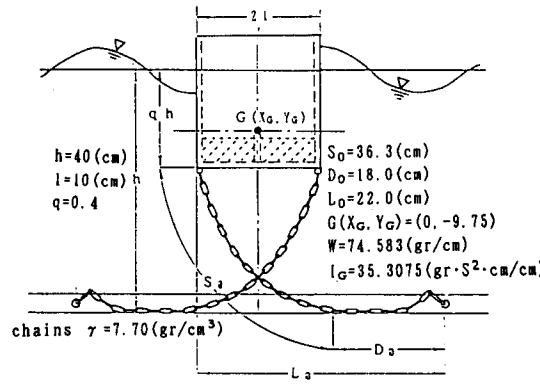

Figure 7. Floating body moored by cross-chains

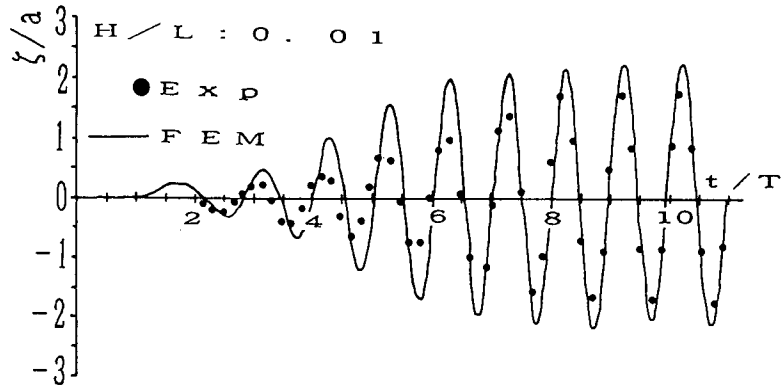

Figure 8. Vertical amplitude ratio of motion of floating body moored by cross-chains

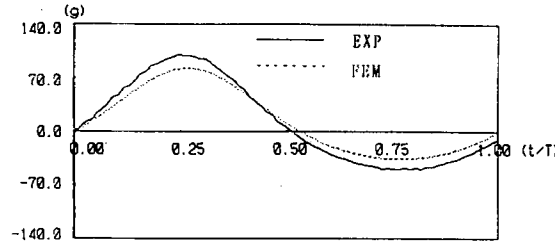

(a) T = 4 sec.

Figure 9. Tension vibration on upper edges of cross-chains

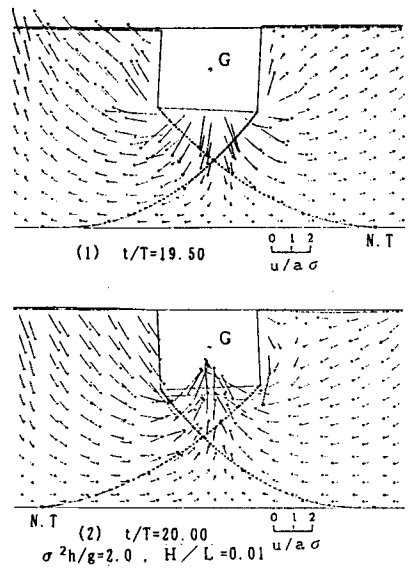

Figure 10. Motion of floating body and time history of velocity fields near floating body

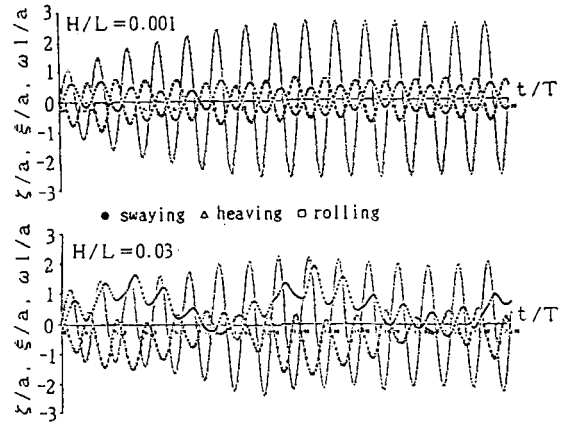

Figure 11. Time history of motion of floating body's centre in regular waves

body moored by cross-springs in regular waves ($\sigma^2 h/g = 2{\cdot}0$). When the steepness of the incident wave (H/L) is small, the motion in each direction is sinusoidal. However, when H/L is large, a finite amplitude of coupled motions is apparent; a low vertical motion ratio and long-period displacement components in swaying and rolling motions are seen.

Figure 12 shows the same history of motion in random waves with a spectrum corresponding to $(\sigma^2 h/g)_{1/3} = 2{\cdot}0$.

A complicated motion appears corresponding to the incident wave characteristic; long-period displacement components in swaying and rolling motions are produced with increasing wave steepness. The drift force acting on a floating body subject to regular waves has so far been treated as a steady force. However, it is evident here that this drift force clearly causes long-period displacement components even in regular waves when the finite amplitude motion including high-order solutions of the potential is computed.

Figure 13 shows the spectrum of each component of the motion of the floating body derived from the results in random waves shown in Figure 12. The vertical axis is the power spectrum of the motion ratio and the horizontal axis is the ratio to frequency f_m of the incident significant waves. When the wave steepness H/L is large, we observe a decrease in the peak value near resonance points ($f/f_m = 1{\cdot}0$) in the heaving motion. We also find that swaying and rolling motions appear at zero

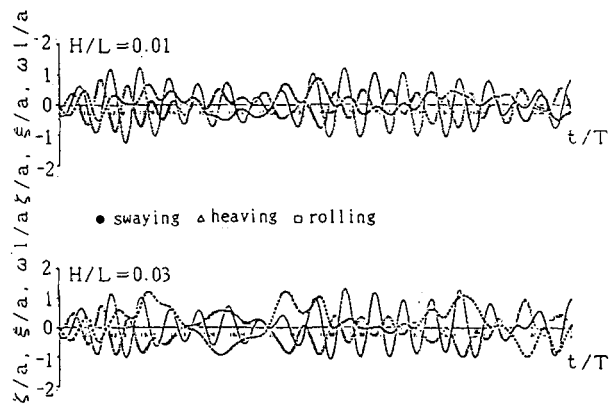

Figure 12. Time history of motion of floating body's centre in random waves

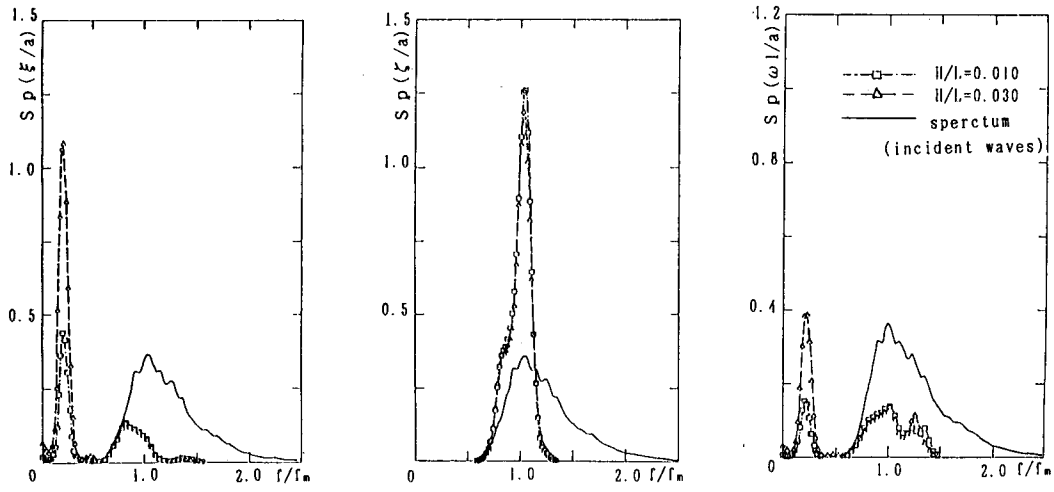

(a) The spectrum of swaying motion (b) The spectrum of heaving motion (c) The spectrum of rolling motion

Figure 13. Spectra of motion of floating body

frequency and at long period, with the peak value increasing with H/L. These indicate both steady drift flow and fluctuating drift flow. In this way we can evaluate the characteristic of this motion by the finite amplitude analysis of the coupled motion of waves and a moored floating body.

5. CONCLUSIONS

The main results obtained by this present non-linear analysis are as follows.

1. When the amplitude of motion of a floating body increases with increasing wave steepness, there is a tendency towards a decrease in amplitude ratio of the floating body motion to the incident wave. This decrease, being one of the characterisics of a non-linear motion to the incident wave. This decrease, being one of the characteristics of a non-linear coupled motion system, cannot be explained only by the drag force arising from the fluid viscosity, because it includes the effect of finite amplitude interactions.
2. In studies based on linear waves theory the drift force acting on a floating body subject to regular waves has been so far treated as a steady force. However, it is shown here that the drift force clearly causes the fluctuation of low-frequency oscillations even in regular waves once the finite amplitude motion is computed.

REFERENCES

1. K. Takikawa and Y. Tabuchi, 'Finite element analysis of wave and a floating body moving boundary problem', *Proc. Coastal Eng., JSCE*, **27**, 1–5 (1980).
2. K. Takikawa and Y. Tabuchi, 'Finite element analysis of nonlinear coupled motion of waves and a floating body', *Proc. Coastal Eng., JSCE*, **33**, 551–555 (1986).
K. Takikawa, Y. Iwagaki and M. Nakagawa, 'Finite element analysis of deformation and internal mechanism of breaking wave on sloping bottom', *Proc. Coastal Eng., JSCE*, **30**, 20–24 (1983).
4. K. Takikawa, H. Furuta and R. Miike, 'Numerical analysis of finite amplitude motion under correlated motion system of waves and a moored floating body', *Jpn. NCTAM, Reprint*, **41**, 97–100 (1991).
5. K. Takikawa and N. H. Kim, 'Open boundary treatment of the finite amplitude wave using the boundary element method', *Eng. Anal. Boundary Elements*, **99–4**, 331–338 (1992).

6. K. Oda, 'The mooring problem of floating structures', *Lecture notes 16th Summer Seminar on Hydraulic Engineering JSCE, B-Z*, 1980.
7. A. Yamasaki, A. Oda, K. Kaku and Y. Nitta, 'Motion of floating body and mooring line tension with dynamic effect', *Proc. JSCE*, **417**(2)–13, 237–244 (1990).